Available online at www.sciencedirect.com
ScienceDirect
Mining Science and Technology 20 (2010) 0178–0182
MINING SCIENCE AND TECHNOLOGY
www.elsevier.com/locate/jcumt

Fissure evolution and evaluation of pressure-relief gas drainage in the exploitation of super-remote protected seams

LIU Hongyong*, CHENG Yuanping, ZHOU Hongxing, WANG Feng, CHEN Haidong

National Engineering and Research Center for Coal Gas Control, China University Mining & Technology, Xuzhou 221008, China

Abstract: Based on nonlinearity contact theory and the geological structure of the Xieqiao Coal Mine in the newly developed Huainan coal field, rock movements, mining fissures and deformation of overlying strata were simulated by using the interface unit of FLAC3D to evaluate the pressure-relief gas drainage in the exploitation of super-remote protected seams. The simulation indicates that the height of the water flowing fractured zone is 54 m in the overlying strata above the protective layer. The maximum relative swelling deformation of the C13 coal seam is 0.232%, while the mining height is 3.0 m and the distance from the B8 roof to the C13 floor is 129 m, which provides good agreement with a similar experiment and in situ results. The feasibility of exploitation of a super-remote protective coal seam and the performance of the pressure-relief gas drainage in a super-remote protected layer are evaluated by comparisons with practice projects. It demonstrates that the relieved gas in the super-remote protected layers could be better drained and it is feasible to exploit the B8 coal seam before the C13 super-remote protected coal seam. The method is applicable for the study of rock movements, mining fissures and deformation of the overburden, using the interface unit to analyze the contact problems in coal mines.

Keywords: protected layers; super remote; contact analysis; gas drainage; numerical simulation

1 Introduction

Clauses 192~193 of the Safety Regulations in Coal Mine (2006 edition) provide as follows: before coal seams with coal and gas outbursts are excavated, protective layers must be excavated first[1]. Excavation technology of protective layers has been proven by many practices, is considered to be an effective way of eliminating coal and gas outbursts and is widely used in a number of mineral fields[2-6]. The excavation of protective layers uses overburden dribbling to release the elastic deformation energy and the gas stored in coal seams and increases permeability of coal seams in certain areas, which could reduce the gas content to eliminate coal and gas outbursts through proper gas drainage.

Clause 48 of the Detailed Rules for Coal and Gas Outburst Prevention provides that the maximum vertical effective distance is no more than 100 m between the protective layer and the protected layer[7]. This is referred to as the super-remote protective layer when the distance to the protected layer is more than 100 m.

Research on the exploitation of super-remote protective layers did not start until the publication of the fifty articles of the gas control experience in coal mines, which provides that gas control should, in first instance, select district measurements, including the exploitation of protective layers and gas drainage[8].

At present, the feasibility of the exploitation of protective seams is largely predicated on the deformation of coal seams, which is a macro reflection of mining fissures. Similar material experiments and numerical simulations are used to study overburden movements and deformations in coal mines. Experiments with similar material can be quite exhausting and the number of measuring points is usually limited and discrete, while the results of most numerical simulations are not suitable in practice since the surface between two layers is taken as agglutination, which cannot simulate separation. Therefore, research and further discussion should be extended to separation and deformation in numerical simulations of protective layers.

For our study, we selected the interface between two layers as contact surfaces, according to a nonlinear contact theory. The deformation and mining fissures of the overburden were computed by using FLAC3D, based on the geological structure of the Xieqiao Coal Mine in a newly developed coal field of Huainan. Finally, the performance of pressure-relief gas drainage under super-remote protected seam ex-

Received 29 August 2009; accepted 12 November 2009
*Corresponding author. Tel: 86 516 83885948
E-mail address: Lhyeven@163.com
doi: 10.1016/S1674-5264(09)60180-0

ploitation was evaluated in a comparison with the practice of protective layers.

The Xieqiao Coal Mine of Huainan is located in a newly developed coal field, covering a thick quaternary sediments layer with complex geological structure, deeply embedded (600~800 m), with significant crustal stress during excavation and high gas pressure and content[3].

Coal seams C13, B11 and B8 are major seams for exploitation in the Xieqiao Coal Mine. The C13 coal seam is a stable and minable coal seams in all areas with a high risk of coal and gas outbursts, an average thickness of 4.72 m, a maximum measured gas pressure of 5.8 MPa, a gas content of 12~22 m^3/t and an original permeability coefficient of 3.92×10^{-2} $m^2/(MPa^2\cdot d)$. The B11 coal seam is also a near stable, minable and very hard coal seam, 66.95 m below C13, with a low risk of coal and gas outbursts, given its low gas content (4~7.5 m^3/t), but not all its areas in this mine field are minable. The B8 coal seam, 86.70 m below B11, is a stable and minable coal seam with low gas content (4~7 m^3/t) and no risk of coal and gas outbursts.

Given the initial geological conditions, it is clear that B11 should be exploited first in order to protect the C13 coal seam, but not all areas in this mine field can be exploited. Therefore, the B8 coal seam has been selected as the protective layer in those sections where B11 is not minable, but the distance from the roof of B8 to the floor of C13 is 153.65 m, clearly beyond the maximum vertical effective distance between the protective and the protected layers provided by Clause 48 of the Detailed Rules for Coal and Gas Outburst Prevention. Therefore, the exploitation of super-remote protective layers and the performance of pressure-relief gas drainage must be predicted before exploiting the B8 coal seam, in order to eliminate the hazards of coal and gas outbursts in the C13 coal seam.

2 Contact analysis between rock (coal) layers

Deformation of coal and rock in mining can be quite different, given the various properties in physical mechanics which leads to the appearance of tensile and shear stresses. Most results of numerical simulation are not suitable for practical use, since the surface between two layers is taken as agglutination which cannot simulate separation. Therefore, we analyzed the mechanical situation between layers by FLAC3D, based on contact theory.

2.1 Theory of contact analysis

It is well known that the augmented Lagrangian method is the most popular numerical method to solve the problem of contact with friction, a highly nonlinear problem[9-10].

Assume that the opening function of two contact objects is g_N. The initial opening is g_0 and the contact conditions are as follows[10]:

$$\begin{cases} g_N = u\cdot n + g_0 \geq 0 \\ P_N(u) = n\cdot\sigma \leq 0 \\ P_N(u)\cdot g_N = 0 \end{cases} \tag{1}$$

where u is the displacement vector of the contact boundary; n the normal direction of the contact boundary; σ the stress of contact objects and $P_N(u)$ the normal stress of the contact boundary.

After introducing the independent Lagrangian coefficients λ_N, λ_T and the penalty program based on the Coulomb friction law and the Kuhn-Tucker condition, we obtain the weak virtual function[10],

$$\begin{cases} G(u\cdot\delta u) = \int_S (-P_N n\cdot\delta u - P_T\cdot\delta u_T)\,\mathrm{d}s \\ P_N = \lambda_N + \Delta_N g_N \\ u_T = \dfrac{1}{\Delta_T}(P_T - \lambda_T) \end{cases} \tag{2}$$

where Δ_N and Δ_T are the penalty parameters; $P_T(u)$ the tangential stress of the contact boundary and u_T the tangential component of the displacement vector.

2.2 Nonlinear analysis of interaction between rock (coal) layers

After excavation of the protective layer, the overburden is in a state of tensile stress, affected by the overburden dead weight and appears as spalling and separation. Spalling is a type of damage of the separation among low-impedance surfaces in media, including shear spalling (dislocation between layers) and extensive spalling (separation). Spalling is generated suddenly when, to some extent, tensile stress accumulates gradually. The dislocation closes in a vertical direction near the stope and becomes the separation far away from the stope.

There are two different kinds of nonlinearity in the interaction of rock or coal layers: 1) a material nonlinearity caused by inelasticity; 2) a static nonlinearity of separation or slip generated in the surfaces of the media.

1) Simulation of material nonlinearity between contact surfaces. We selected plastic action as the elastic-perfect plasticity and adopted the Hoek-Brown failure criterion and other related stream criteria[11].

2) Simulation of static nonlinearity in contact surfaces. We used the interface unit of the FLAC3D program to analyze contact problems. FLAC3D is a three-dimensioned program which computes explicit finite-differences in engineering mechanics. It offers a wide range of abilities to solve complex problems in mechanics, especially in geomechanics. The program has many basic built-in material failure criteria, such as the Drucker-Prager, Mohr-Coulomb, strain-

hardening/softening, double-yield, modified Camclay and Hoek-Brown. The explicit Lagrangian calculation scheme and the mixed-discretization zoning technique used in FLAC3D ensure that plastic collapse and flows are modeled accurately[11].

We generated wrap 1 as the contact surface on the soft layer of rock or coal layers and wrap 2 as the target surface on the hard layer to simulate cohesion, sliding, separation of the interfaces by choosing appropriate parameters.

3 Numerical simulation

3.1 Establishment of numerical model

The computation models were based on the geological features of the newly developed Huainan coal field. In the simulation, the distance from the B8 roof to the C13 floor is 129 m, 43 times the mining height. The geometric and physical/mechanical parameters of the coal and rock seams in the model are shown in Table 1.

Taking account of the structural characteristics, the requirements for precision and the obvious impact on the rock in particular regions of excavation, the dimensions for the computation models are 300 m×216 m with an excavation length of 100 m in the B8 coal seam. The boundary of the model, was fixed except the bottom and the top, where has no normal displacement and applying the weight of incumbent rock seams.

For our calculations, we made the following assumptions: the sandwiched rock is an isotropic continuous elastic-plastic material for each layer; we ignored the effect of major factors on the final stress distribution, such as concentrated stress, tectonic stress, temperature stress and additional stress caused by gas[10]. The balance of the original ground stress affected by the gravity of the overburden in the computation model was achieved before excavation. We used generate separate and interface *n* wrap to simulate the interface activities between the layers.

Table 1 Geometric and physical/mechanical parameters of coal and rock seams in the model

No.	Main ingredient	Thickness (m)	Unit weight γ (kN/m^3)	Young's modulus E (GPa)	Poisson ratio v	Uniaxial strength σ_c (MPa)
1	Quartz sandstone	9	24.99	43	0.33	53.6
2	Siltstone	15	25.09	14.5	0.27	60.5
3	Calcilutite	12	23.52	19.0	0.35	35.0
4	Sandy mudstone	6	25.28	15.6	0.26	38.4
5	C13 coal seam	5	13.72	4.8	0.39	15.0
6	Sandy mudstone	5	25.28	15.6	0.26	38.4
7	Packsand	6	24.50	27.4	0.35	60.8
8	Sandy mudstone	18	25.28	15.6	0.26	38.4
9	Sandstone	8	26.17	39.3	0.38	75.9
10	Mudstone	4	23.52	13.0	0.23	26.8
11	Packsand	5	24.50	27.4	0.35	60.8
12	Sandy mudstone	9	25.28	15.6	0.26	38.4
13	B11 coal seam	2	13.72	4.8	0.39	20.0
14	Mudstone	4	23.52	13.0	0.23	26.8
15	Quartz sandstone	16	24.99	43	0.33	53.6
16	Sandy mudstone	17	25.28	15.6	0.26	38.4
17	Packsand	5	24.50	27.4	0.35	60.8
18	Sandy mudstone	13	25.28	15.6	0.26	38.4
19	Quartz sandstone	10	24.99	43	0.33	53.6
20	Sandy mudstone	7	25.28	15.6	0.26	38.4
21	B8 coal seam	3	13.72	4.8	0.39	20.0
22	Sandy mudstone	17	25.97	15.6	0.26	63.3
23	Sandstone	20	26.17	39.3	0.38	75.9

3.2 Analysis of the simulation

The parts of the overburden near the stope appear as bending deformation and are separated from the overburden after the excavation of the protective layers. Fig. 1 shows the separation and the horizontal stress of the overburden upon the stope.

We can analyze the separation from the distribution of horizontal stress since it is caused by shear and tensile stress. The separation appears in the range of 54 m in the overburden near the stope, as shown in Fig. 1. The separation volume is different from the thickness and main ingredients of correlated rock layers.

The height of the caving zone above the protective layer is 18 m, six times that of the mining height. The height of the fractured zone is 36 m, twelve times the mining height, which agrees with the empirical value[12]. In general, the sum of the caving zone and the fractured zone are known as the water flowing fractured zone. However, the height of the water flowing fractured zone is only 54 m, less than the distance from the roof of B8 to the floor of C13, thus

the protected layer C13 lays in the curve subsidence zone. As shown in Fig. 2, the pressure-relief angles of the model along the strike are 76°, both at the open-off cut and the working face after exploitation of the B8 seam.

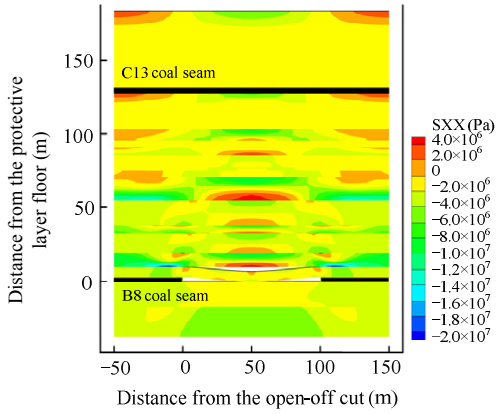

Fig. 1 Separation and horizontal stress of overburden upon the stope

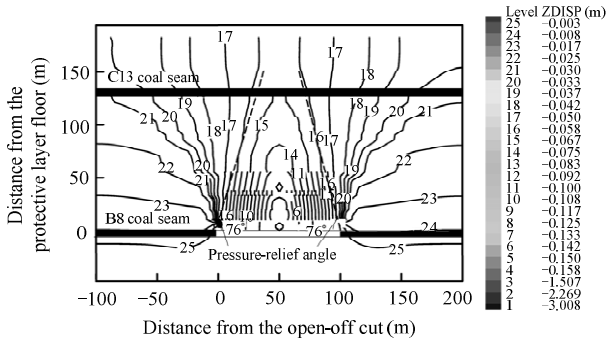

Fig. 2 Vertical display of overburden

The protected layers are compressed 5~50 m away from the open-off cut in the pillar. The maximum relative compressed deformation of C13 is 0.026% (1.7 mm). The relative deformation is expanded around the workface boundary to 0.016%, since the shear stress generates horizontal fissures. The swelling deformation achieves 0.2% (8 mm) at 32 m distance away from the open-off cut and 0.2325 (9.3 mm) at 47 m, as shown in Fig. 3. The range of the protected zone becomes smaller when the vertical distance is further away from the protective layer.

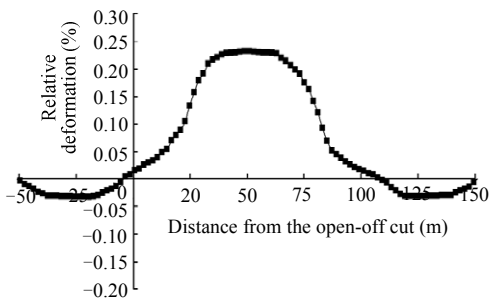

Fig. 3 Deformation curve of C13 at various distances from the open-off cut in numerical simulation

4 Results of a similar experiment and in-situ measurements

A similar experiment was performed in order to assess the exploitation feasibility and the performances of pressure-relief gas drainage, optimizing the effect of protective layers in mining. The result of that experiment is shown in Fig. 4.

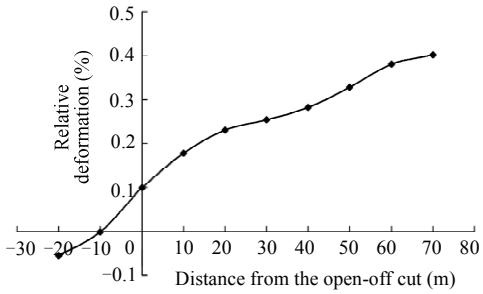

Fig. 4 Relative deformation curve of C13 in similar experiment

The height of caving zone above the protective layer is 13.4 m and the height of the fractured zone 27.8 m, respectively 4.5 and 9.1 times the mining height. The maximum compressed and swelling deformation of the C13 seam are 2.9 and 20.9 mm, 0.055% and 0.402% of the thickness of the protected layer. The deformation curve of the protected layers of C13 is shown in Fig. 4.

However, the micro-separation and fracture could not be found for the macroscopic measurement. Hence, the results of the deformation and height of the water flowing fractured zone are smaller than from numerical simulation, with the in situ measurements are larger than those of the experimental and numerical simulations. From this comparison, we can conclude that the numerical simulation agrees with practice experience and is within the same order of magnitude.

According to the result from practical projects, the permeability of the seam will increase more than 100 times and the pressure-relief gas drainage will be very satisfactory when the relative deformation of the protective layers reaches 0.1%~0.2%.

In the Xieqiao Coal Mine, the maximum relative swelling deformation of the C13 seam reaches 0.232% (9.3 mm) with a mining height of 3 m and a distance between protective layer and protected layer of 129 m. As a result, it can be predicted that the permeability of seam C13 will increase more than 10 times. The pressure-relief gas drainage is highly satisfactory after the exploitation of the B8 coal seam. Therefore, it is feasible to exploit the B8 coal seam as pressure relief for C13. It also demonstrates the feasibility of taking the interface between two layers as contact surfaces to analyze rock movements, mining fissures and deformation affected by the exploitation of the protective layer[14-16] (Table 2).

Table 2 Changes of protected layers affected by protective layers in some coal mines[13]

Name	Deep (m)	Distance from the protective layer (m)	Protective layer thickness (m)	Maximum relative deformation (%)	Times of gas emission	Times of permeability coefficient	Gas drainage ratio (%)	Memo
Moxinpo	470	80	0.55	0.31	50	300		
Guanshan	400	69	1.45	0.069	2000			Under protected layers
Yongshan	280	53	2.7	0.23	69	175		
Yutianpu	200	36	1.5	0.17	12			
Panji	600	66.7	1.9	2.64		2880	>6.0	Upper protected layers
Xieji	730	70	2	0.4			>6.5	

5 Conclusions

1) Within 54 m of the overburden upon the stope, separation appears after the excavation of the protective layer B8. The separation volume is different from the thickness and main ingredients of the correlated layers. The maximum relative compressed deformation and swelling deformation of C13 are 0.026% (1.7 mm) and 0.232% (9.3 mm) respectively, which are basically consistent with those of a similar experiment and in situ results.

2) For all practical purposes, the exploitation of the B8 coal seam before C13 is feasible. The gas drainage can be very satisfactory with a mining height of 3.0 m and a distance between the protective layer and the protected layer of 129 m in the Xieqiao coal mine.

3) It is feasible to take the interface between the two layers as the contact surface for rock movements, mining fissures and deformation affected by the exploitation of the protective layer.

Acknowledgments

The authors are grateful to the National Basic Research Program of China (No.2005CB221503), the Major Program of the National Natural Science Foundation of China (No.70533050) and the National Natural Science Foundation of China (No.50674089) for their support.

References

[1] State Administration of Coal Mine Safety. *Safety Regulations in Coal Mine*. Beijing: China Coal Industry Publishing House, 2007. (In Chinese)

[2] Yu Q X, Cheng Y P, Jiang C L, Zhou S N. Principles and applications of exploitation of coal and pressure relief gas in thick and high gas seams. *Journal of China University of Mining & Technology*, 2004, 33(2): 128-131. (In Chinese)

[3] Cheng Y P, Yu Q X, Yuan L. Gas extraction techniques and movement properties long distance and pressure relief rock mass upon exploited coal seam. *Journal of Liaoning Technical University*, 2003, 22(4): 483-486. (In Chinese)

[4] Cheng Y P, Yu Q X, Yuan L. Experimental research of safe and high efficient exploitation of coal and pressure relief gas in long distance. *Journal of China University of Mining & Technology*, 2004, 33(2): 132-136. (In Chinese)

[5] Wang L, Cheng Y P, Li F R, Wang H F, Liu H B. Fracture evolution and pressure relief gas drainage from distant protected coal seams under an extremely thick key stratum. *Journal of China University of Mining & Technology*, 2008, 18(2): 182-186.

[6] Hu G Z, Wang H T, Fan X G, Li X H, Deng Y, Shen Y H. Gas pressure investigation on protection region of up-protective layer of pitching oblique mining. *Journal of China University of Mining & Technology*, 2008, 37(3): 328-332. (In Chinese)

[7] State Coal Industry Administration of China. *Detailed Rules for Coal and Gas Outburst Prevention*. Beijing: China Coal Industry Publishing House, 1993. (In Chinese)

[8] National Development and Reform Commission. *The fifty Articles of the Gas Control Experience in Coal Mines*. Beijing: China Coal Industry Publishing House, 2005. (In Chinese)

[9] Wang L, Cheng Y P, Li F R, Wang H F, Liu H B. Fracture evolution and pressure relief gas drainage from distant protected coal seams under an extremely thick key stratum. *Journal of China University of Mining & Technology*, 2008, 18(2): 182-186.

[10] Liu J, Wang H, Shi G Y. Application contact analysis in deep foundation layer anti-sliding stability numerical analysis of gravity dam. *Water Resources & Hydropower of Northeast China*, 2002, 3(4): 14-17. (In Chinese)

[11] Zhang B S, Kang L X, Yang S S. Numerical simulation on roof separation and deformation of full seam roadway with stratified roof and large section. *Journal of Mining & Safety Engineering*, 2006, 23(3): 264-267. (In Chinese)

[12] Ma L Q, Zhang D S, Jing S G. Numerical simulation analysis by solid-liquid coupling with 3DEC of dynamic water crannies in overlying strata. *Journal of China University of Mining and Technology*, 2008, 18(3): 347-352.

[13] Ren Q, Liu W T. Numerical simulation analysis of overburden crack belt developing disciplinary. *Journal of Safety and Environment*, 2006, 6(7): 76-78. (In Chinese)

[14] Yu B F. *Cognition and Practice on the Exploitation of the Protective Layers*. Beijing: China Coal Industry Publishing House, 1986. (In Chinese)

[15] Liu L, Cheng Y P, Wang H F. Principle and engineering application of pressure relief gas drainage in low permeability outburst coal seam. *Mining Science and Technology*, 2009, 19(3): 342-345.

[16] Liu H B, Cheng Y P, Song J C. Pressure relief, gas drainage and deformation effects on an overlying coal seam induced by drilling an extra-thin protective coal seam. *Mining Science and Technology*, 2009, 19(6): 724-729.